American Mineralogist, Volume 95, pages 188–191, 2010

LETTER

Hibonite-(Fe), $(Fe,Mg)Al_{12}O_{19}$, a new alteration mineral from the Allende meteorite

CHI MA*

Division of Geological and Planetary Sciences, California Institute of Technology, Pasadena, California 91125, U.S.A.

ABSTRACT

Hibonite-(Fe), $(Fe,Mg)Al_{12}O_{19}$, is the Fe^{2+}-dominant analog of hibonite $CaAl_{12}O_{19}$, discovered in a highly altered Ca-,Al-rich refractory inclusion from the Allende meteorite. It occurs as scattered micrometer-sized single crystals within an aggregate of hercynite $(Fe,Mg)Al_2O_4$, adjacent to nepheline, ilmenite, ferroan spinel, perovskite, and hibonite. The mean chemical composition determined by electron microprobe analysis of hibonite-(Fe) is Al_2O_3 90.05 wt%, FeO 3.60, SiO_2 2.09, MgO 1.61, Na_2O 0.55, CaO 0.28, TiO_2 0.04, V_2O_3 0.02, sum 98.25, corresponding to an empirical formula of $(Fe^{2+}_{0.34}Mg_{0.27}Na_{0.12}Al_{0.11}Ca_{0.03})_{\Sigma 0.87}(Al_{11.77}Si_{0.23})_{\Sigma 12.00}O_{19}$. Hibonite-(Fe) is hexagonal, $P6_3/mmc$; $a = 5.613$ Å, $c = 22.285$ Å, $V = 608.0$ Å^3 and $Z = 2$. Its electron backscatter diffraction pattern is a good match to that of the hibonite structure. Hibonite-(Fe) is apparently a secondary alteration product formed by iron-alkali-halogen metasomatism, whereas hibonite is a primary refractory phase.

Keywords: Hibonite-(Fe), $(Fe,Mg)Al_{12}O_{19}$, a new Al-rich mineral, refractory inclusion, secondary alteration, Allende meteorite, carbonaceous chondrite, nanomineralogy

INTRODUCTION

Nanomineralogy is the study of Earth and planetary materials at nano-scales, focused on characterizing nanofeatures (like inclusions, exsolution, zonation, coatings, pores) in minerals and revealing nanominerals and nanoparticles (Ma 2008). During a nanomineralogy investigation of the Allende CV3 meteorite at Caltech, new refractory minerals and new minerals in refractory inclusions have been discovered at micro- to nano-scales, including allendeite ($Sc_4Zr_3O_{12}$) and hexamolybdenum (Mo,Ru,Fe) (Ma et al. 2009a), monipite (MoNiP) (Ma et al. 2009b), tistarite (Ti_2O_3) (Ma and Rossman 2009a), davisite ($CaScAlSiO_6$) (Ma and Rossman 2009b), and grossmanite ($CaTi^{3+}AlSiO_6$) (Ma and Rossman 2009c). Each new phase adds a new voice toward understanding the processes that occurred in the early solar system.

This paper describes a new Al-rich mineral, $(Fe,Mg)Al_{12}O_{19}$, identified in an Allende Ca-,Al-rich refractory inclusion (CAI). Electron-microprobe, high-resolution SEM, electron backscatter diffraction (EBSD), and mico-Raman analyses have been used to characterize its composition and structure and associated minerals. Synthetic $FeAl_{12}O_{19}$–$(Fe,Mg)Al_{12}O_{19}$ phases are not known in the field of materials science. Reported here is the first occurrence of $(Fe,Mg)Al_{12}O_{19}$ in nature, as a new alteration mineral in a CAI from a primitive meteorite.

MINERAL NAME AND TYPE MATERIAL

The new mineral and its name have been approved by the Commission on New Minerals, Nomenclature and Classification of the International Mineralogical Association (IMA 2009-027). The name, hibonite-(Fe), is for the composition, the mineral being the Fe^{2+}-dominant analog of hibonite $CaAl_{12}O_{19}$. Holotype material (Caltech Allende12A section D) has been deposited in the Smithsonian Institution's National Museum of Natural History, Washington, D.C., and is cataloged under USNM 7554.

OCCURRENCE, ASSOCIATED MINERALS, AND ORIGIN

Micrometer-sized hibonite-(Fe) occurs as scattered single crystals surrounded by hercynite, along with hibonite, perovskite, ferroan spinel, ilmenite, and nepheline in the central area of a highly altered CAI from the Allende meteorite (Fig. 1). Ferroan spinel, anorthite, nepheline, hedenbergite, diopside, ilmenite, and perovskite are present in the mantle and rim areas of the CAI. Hibonite-(Fe), hercynite, ferroan spinel, ilmenite, nepheline, anorthite, hedenbergite, and diopside appear to be secondary phases based on their petrographic textures, whereas hibonite and perovskite are primary phases of the CAI. Hibonite ($CaAl_{12}O_{19}$) is irregular to lath-shaped, 2~12 μm in size, containing a small amount of Mg^{2+} and Ti^{4+} in the Al site (Table 1). Perovskite is irregular to subhedral, 3~10 μm in diameter, often coated by ilmenite, with an empirical formula of $Ca_{1.00}(Ti_{0.98}Al_{0.02}Fe_{0.01})O_3$. The occurrence of nepheline, ferroan spinel and hedenbergite indicates a secondary alteration by iron-alkali-halogen metasomatism to which the primary CAI was subjected. Trace amount of Cl was detected in some nepheline and anorthite domains where sodalite nano-inclusions might be present. Ferroan spinel is one of the dominant phases along with anorthite and nepheline in the CAI, irregular to lath shaped, <15 μm in size, with Fe/(Mg+Fe) ratios ranging from 0.16 to 0.24. The original primary phase assemblage might be hibonite–perovskite–grossmanite–MgAl spinel–melilite.

This CAI is about 900 μm in size in the section plane with cavities inside, surrounded by matrix (mainly olivine and troilite), prepared from a 1 cm Allende specimen at Caltech. The Allende meteorite, which fell at Pueblito de Allende, Chihuahua, Mexico, on February 8, 1969, is a CV3 carbonaceous chondrite.

* E-mail: chi@gps.caltech.edu

0003-004X/10/0001–188$05.00/DOI: 10.2138/am.2010.3365

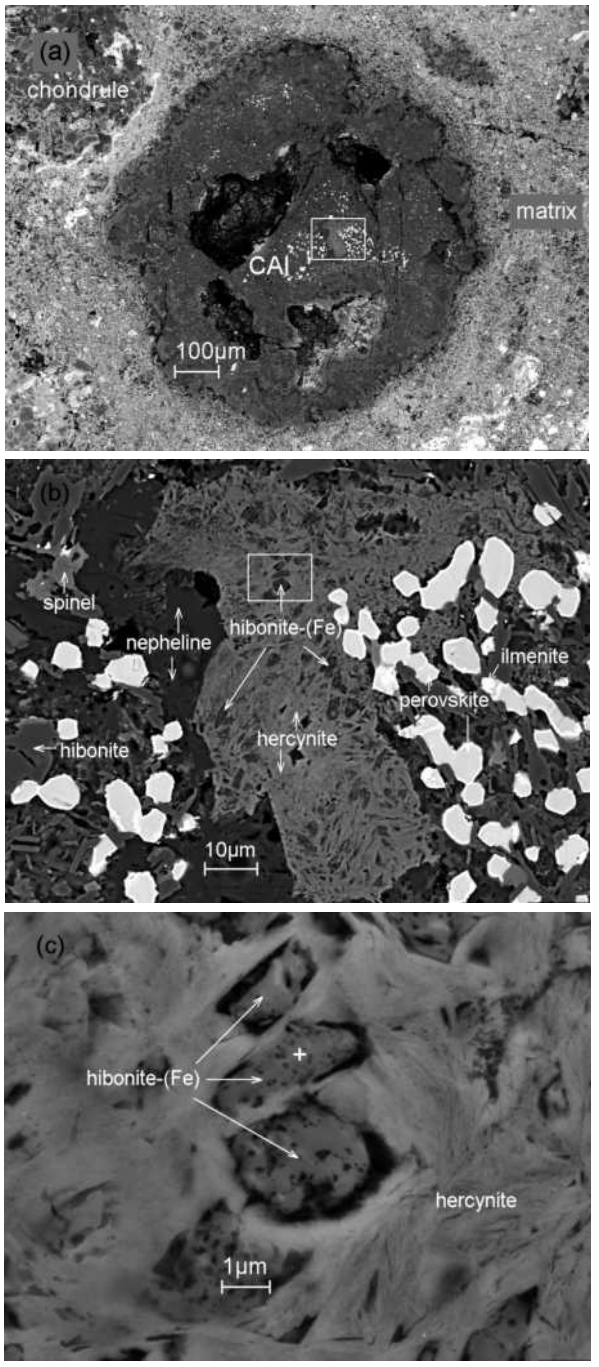

FIGURE 1. (**a**) Back-scatter electron image of a highly altered CAI in Allende section USNM 7554; (**b**) enlarged BSE image showing hibonite-(Fe) within hercynite, along with hibonite, spinel, perovskite, ilmenite, and nepheline; (**c**) further enlarged BSE image showing hibonite-(Fe) and surrounding hercynite. The cross marks where the EBSD pattern (shown in Fig. 2) was collected.

APPEARANCE, PHYSICAL AND OPTICAL PROPERTIES

The individual hibonite-(Fe) crystals are 1–4 μm in size (type material). The mineral appears to contain nano-pores (Fig. 1c). Color, streak, luster, hardness, tenacity, cleavage, fracture, density, and optical properties were not determined because of the small grain size of the mineral and the limited amount of material available. The density, calculated from the empirical formula, is 3.61 g/cm^3. It is non-fluorescent under an electron beam. In the section, the crystal grains are subhedral. No forms or twinning were observed. The *c*:*a* ratio calculated from the unit-cell parameters is 1:3.970.

TABLE 1. The electron microprobe analytical results for hibonite-(Fe), nearby hibonite, and associated hercynite in the CAI

Constituent	Hibonite-(Fe) wt%	n = 7 S.D.	Hibonite wt%	n = 10 S.D.	Hercynite wt%	n = 8 S.D.
Al_2O_3	90.05	0.81	77.68	1.31	65.37	1.09
FeO	3.60	0.35	0.50	0.14	19.85	2.74
SiO_2	2.09	0.46	0.40	0.23	2.74	0.59
MgO	1.61	0.14	4.23	0.34	8.60	1.35
Na_2O	0.55	0.23	0.05	0.07	0.63	0.12
CaO	0.28	0.03	8.51	0.16	0.60	0.11
TiO_2	0.04	0.01	7.90	0.83	0.11	0.04
V_2O_3	0.02	0.01	0.18	0.03	0.02	0.01
MnO	b.d.		b.d.		0.07	0.03
K_2O	b.d.		b.d.		0.02	0.01
Total	98.25		99.45		98.01	
Number of ions on the basis of 19 O atoms for hibonite-(Fe) and hibonite, 4 O atoms for hercynite						
Al	11.860		10.469		2.028	
Fe^{2+}	0.337		0.048		0.438	
Si	0.234		0.046		0.072	
Mg	0.268		0.720		0.337	
Na	0.119		0.011		0.032	
Ca	0.034		1.042		0.017	
Ti^{4+}	0.004		0.679		0.002	
V	0.002		0.016		0.000	
Mn	–		–		0.002	
K	–		–		0.001	
Cation sum	12.858		13.031		2.929	

Notes: b.d. = below detection limit, 0.039 wt% MnO, 0.012 wt% K_2O.

CHEMICAL COMPOSITION

Quantitative elemental microanalyses were conducted with a JEOL 8200 electron microprobe operated at 15 kV and 10 nA in a focused beam mode. Standards for the analysis were spinel (Al*K*α, Mg*K*α), anorthite (Ca*K*α, Si*K*α), synthetic fayalite (Fe*K*α), synthetic Mn_2SiO_4 (Mn*K*α), TiO_2 (Ti*K*α), V_2O_3 (V*K*α), albite (Na*K*α), and microcline (K*K*α). Analyses were processed with the CITZAF correction procedure (Armstrong 1995). Electron microprobe analyses of the type material (the larger crystals, 3~4 μm in diameter in the section plane) were carried out using WDS mode and repeated for the reproducible and reliable results (Table 1). Nano-pores in the crystals may be the cause for the slightly low sum 98.25 wt%. No other elements with atomic number greater than 4 were detected by WDS scans. The empirical formula, based on 19 O apfu, is: $(Fe^{2+}_{0.34}Mg_{0.27}Na_{0.12}Al_{0.11}Ca_{0.03})_{\Sigma 0.87}(Al_{11.77}Si_{0.23})_{\Sigma 12.00}O_{19}$, where Fe is assumed to be 2+. The general formula is $(Fe,Mg)Al_{12}O_{19}$ and the Fe end-member formula is $FeAl_{12}O_{19}$, which requires FeO 10.51, Al_2O_3 89.49, total 100.00 wt%.

CRYSTALLOGRAPHY

Crystallography by EBSD at a sub-micrometer scale was carried out using the methods described in Ma and Rossman (2008, 2009a) with an HKL EBSD system on a ZEISS 1550VP scanning electron microscope, operated at 20 kV and 6 nA in a focused beam with a 70° tilted stage. The structure was determined and cell constants were obtained by matching the experimental EBSD patterns with the structures of hibonite (Kato and Saalfeld 1968; Harder and Mueller-Buschbaum 1977; Bermanec et al. 1996) and corundum (Pillet et al. 2001). The HKL software automatically suggests indexing solutions ranked by the lowest "mean

angular deviation" (MAD). MAD numbers <1 are considered desirable for accurate solutions. The solution selected in this study was the highest ranked solution and exhibited a MAD number below 0.5.

The EBSD patterns can be indexed only by the hibonite structure to give a best fit based on unit-cell data from hibonite (Bermanec et al. 1996) (Fig. 2), showing a hexagonal structure, space group $P6_3/mmc$, $a = 5.613$ Å, $c = 22.285$ Å, $V = 608.0$ Å^3, and $Z = 2$ with the mean angular deviations as low as 0.42°. No errors are stated because the cell parameters are taken directly from the data of the matching phase in Bermanec et al. (1996).

To protect the holotype material, the transmission electron microscope was not used to investigate its structure because that would require a destructive focused ion-beam sample preparation. The hibonite-(Fe) crystals, studied by electron backscatter diffraction, are too small for conventional single-crystal or powder XRD study. X-ray powder diffraction data (Cu$K\alpha$1) are calculated from the cell parameters from Bermanec et al. (1996) with the empirical formula of the type hibonite-(Fe) from this study (Table 1) using Powder Cell version 2.4 (2000). The strongest X-ray powder diffraction lines are [*d*-spacing in Å, (*I*), *hkl*] 5.571 (62) (004), 2.807 (100) (110), 2.663 (48) (107), 2.506 (54) (114), 2.229 (43) (0010), 2.228 (51) (204), 2.134 (65) (205), and 1.403 (61) (220).

The EBSD pattern of nearby primary hibonite (Fig. 3) shows sharper diffraction bands with more details than that of hibonite-(Fe), indicating a well-ordered structure. The mean chemical composition of primary hibonite by electron microprobe analysis (Table 1) shows an empirical formula of $(Ca_{1.04}Na_{0.01})_{\Sigma 1.05}(Al_{10.47}Mg_{0.72}Ti_{0.68}Si_{0.05}Fe_{0.05}V_{0.02})_{\Sigma 11.99}O_{19}$. The EBSD bands with less details from hibonite-(Fe) may be due to cation disordering of Fe, Mg, Na, Al, and Ca in the Fe site in its structure.

Spectroscopic properties

Raman microanalysis was carried out using the methods described in Ma and Rossman (2008, 2009a). A Renishaw M1000 micro-Raman spectrometer system was used. Raman analysis gave no indication of either H_2O or CO_2 in hibonite-(Fe). Micro-Raman analyses show that the spectrum of hibonite-(Fe) (using a 514.5 nm laser) is close to that of nearby primary hibonite (Fig. 4), showing main features at 1067, 1014, 748, 728, 490, and 432 cm^{-1}.

Associated hercynite

Hercynite $(Fe,Mg)Al_2O_4$ that hosts hibonite-(Fe) occurs as an aggregate (Fig. 1b), as revealed by EBSD analysis. It appears in a mat form, consisting of unusual lath- or fiber-like crystals at micro- to nano-scales (Fig. 1c). Its mean chemical composition by electron microprobe analysis (Table 1) reveals Fe/(Fe+Mg) atomic ratio = 0.57. It contains 2.74 wt% SiO_2 and trace amounts of Na and Ca, which may be contaminations from likely nepheline nano-inclusions in the aggregate. EBSD patterns of single hercynite crystals are weak, as illustrated in Figure 5, implying a disordered crystal structure. The patterns match the $Fd\bar{3}m$ spinel structure. The Raman modes of hercynite are quite different from those of hibonite-(Fe) and hibonite (Fig. 4), and show broad features at 1608 and 1345 cm^{-1} and a peak at 406 cm^{-1}. The same features observed in the Raman spectrum of hibonite-(Fe) are likely contaminations from surrounding or underlying hercynite.

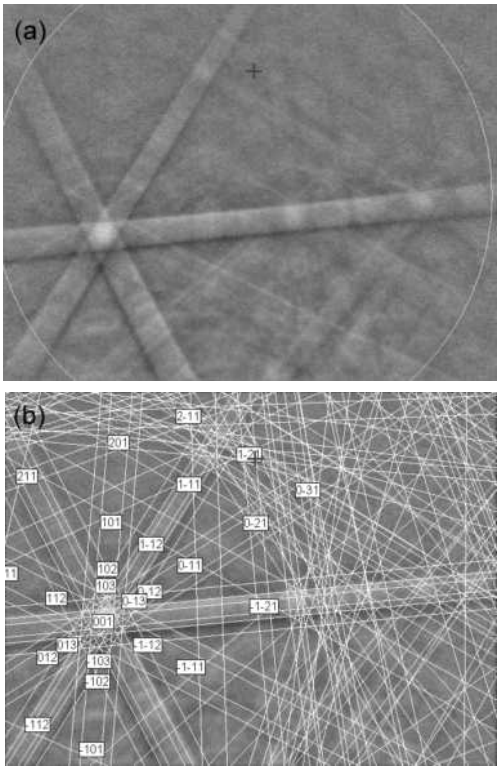

Figure 2. (**a**) EBSD pattern of the labeled hibonite-(Fe) crystal (marked with a cross) in Figure 1c; (**b**) the pattern indexed with the $P6_3/mmc$ hibonite structure.

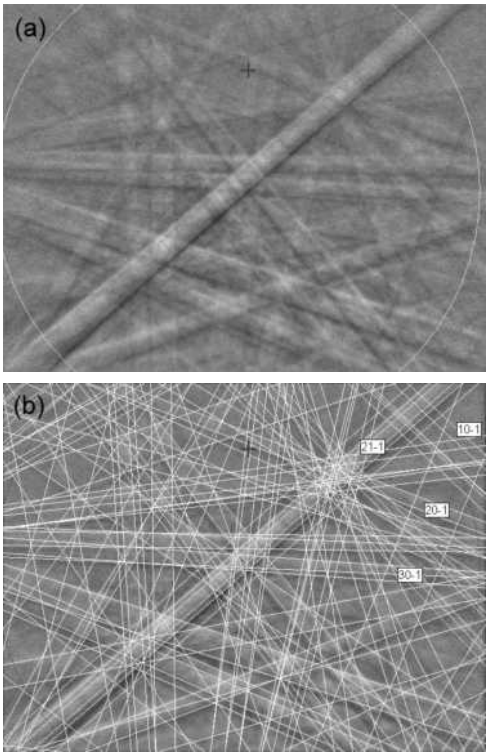

Figure 3. (**a**) EBSD pattern of a nearby primary hibonite $CaAl_{12}O_{19}$ crystal; (**b**) the pattern indexed with the $P6_3/mmc$ hibonite structure.

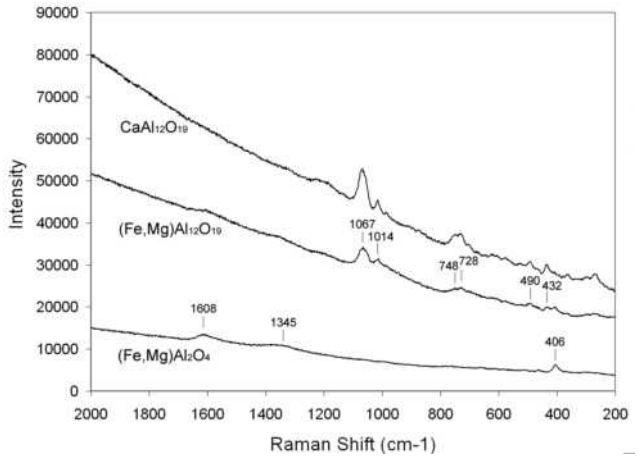

FIGURE 4. Raman spectra of hibonite-(Fe) $(Fe,Mg)Al_{12}O_{19}$, nearby hibonite $CaAl_{12}O_{19}$, and associated hercynite $(Fe,Mg)Al_2O_4$ in the Allende CAI, collected under same conditions.

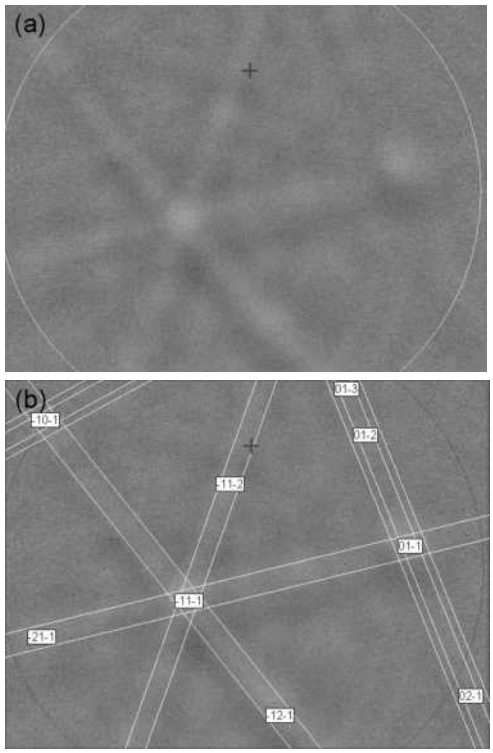

FIGURE 5. (**a**) EBSD pattern of a hercynite $(Fe,Mg)Al_2O_4$ crystal; (**b**) the pattern indexed with the $Fd\bar{3}m$ spinel structure.

DISCUSSION

Hibonite-(Fe) is a new member of the plumboferrite group, the Fe^{2+}-dominant analog of hibonite $CaAl_{12}O_{19}$. It is a β-alumina phase with Fe^{2+} as the intercalated cation, rather than Ca as in conventional hibonite.

Hibonite is a common primary phase in refractory inclusions, ranking second in the condensation sequence after corundum (Grossman 1972), and was among the first major solids formed in the solar nebula. In contrast, hibonite-(Fe) is a rare secondary alteration phase, apparently formed by iron-alkali-halogen metasomatism along with hercynite, replacing primary phase(s) such as hibonite in CAI. A simple scenario for the breakdown of hibonite in a hot Fe- and Mg-rich vapor to produce hibonite-(Fe) and hercynite, is expressed as

$$CaAl_{12}O_{19} + (FeO,MgO)\ (gas) = (Fe,Mg)Al_{12}O_{19} + CaO,$$
$$(Fe,Mg)Al_{12}O_{19} + 5(FeO,MgO)\ (gas) = 6(Fe,Mg)Al_2O_4.$$

Given time, during alteration hibonite-(Fe) would likely be replaced by $(Fe,Mg)Al_2O_4$, as indicated by its petrographic texture. CaO from the primary hibonite could have contributed to the formation of anorthite, diopside, and hedenbergite.

Late-stage alteration often appears in CV3 chondrites, and probably occurred in the nebular environment as well as on the parent body (Krot et al. 1995; Brearley 2005). The heterogeneous distribution of anhydrous alteration phases in this hibonite-(Fe) containing CAI and nearby CAIs implies the secondary phases formed by reaction of primary CAI minerals with a nebular gas. No phyllosilicates were observed in this CAI. This, plus the absence of water in its structure, suggests that aqueous alteration is not likely to have contributed to the formation of hibonite-(Fe).

ACKNOWLEDGMENTS

The Caltech Analytical Facility at the Division of Geological and Planetary Sciences is supported, in part, by grant NSF EAR-0318518 and the MRSEC Program of the NSF under DMR-0080065. The author thanks George Rossman for assistance with micro-Raman analysis, John Beckett for discussion on the formation and alteration of CAIs, Christine Floss and Steve Simon for constructive reviews of this manuscript.

REFERENCES CITED

Armstrong, J.T. (1995) CITZAF: A package of correction programs for the quantitative electron microbeam X-ray analysis of thick polished materials, thin films, and particles. Microbeam Analysis, 4, 177–200.

Bermanec, V., Holtstam, D., Sturman, D., Criddle, A.J., Back, M.E., and Scavnicar, S. (1996) Nezilovite, a new member of the magnetoplumbite group, and the crystal chemistry of mognetoplumbite and hibonite. Canadian Mineralogist, 34, 1287–1297.

Brearley, A.J. (2005) Nebular versus parent-body processing. In A.M. Davis, Ed., Meteorites, Comets, and Planets, 1, p. 247–268. Treatise on Geochemistry, Elsevier, Amsterdam.

Grossman, L. (1972) Condensation in the primitive solar nebula. Geochimica et Cosmochimica Acta, 49, 2433–2444.

Harder, M. and Mueller-Buschbaum, H. (1977) $CaFe_6Al_6O_{19}$ mit magnetoplumbitstruktur. Zeitschrift für Naturforschung, Teil B. Anorganische Chemie, Organische Chemie, 32, 833–834.

Kato, K. and Saalfeld, H. (1968) Verfeinerung der kristallstruktur von $CaO(Al_2O_3)_6$. Neues Jahrbuch für Mineralogie. Abhandlungen, 109, 192–200.

Krot, A.N., Scott, E.R., and Zolensky, M.E. (1995) Mineralogical and chemical modification of components in CV3 chondrites: Nebular or asteroidal processing? Meteoritics, 30, 748–775.

Ma, C. (2008) Discovering new minerals in the early solar system: A nano-mineralogy investigation. Eos Transactions AGU, 89, Fall Meeting Supplement, Abstract MR12A-01.

Ma, C. and Rossman, G.R. (2008) Barioperovskite, $BaTiO_3$, a new mineral from the Benitoite Mine, California. American Mineralogist, 93, 154–157.

——— (2009a) Tistarite, Ti_2O_3, a new refractory mineral from the Allende meteorite. American Mineralogist, 94, 841–844.

——— (2009b) Davisite, $CaScAlSiO_6$, a new pyroxene from the Allende meteorite. American Mineralogist, 94, 845–848.

——— (2009c) Grossmanite, $CaTi^{3+}AlSiO_6$, a new pyroxene from the Allende meteorite. American Mineralogist, 94, 1491–1494.

Ma, C., Beckett, J.R., and Rossman, G.R. (2009a) Allendeite and hexamolybdenum: two new ultra-refractory minerals in Allende and two missing links. 40th Lunar and Planetary Science Conference, Abstract 1402.

——— (2009b) Discovery of a new phosphide mineral, monipite (MoNiP), in an Allende Type B1 CAI. Meteoritics & Planetary Science, 44, Supplement, A127.

Pillet, S., Souhassou, M., Lecomte, C., Schwarz, K., Blaha, P., Rerat, M., Lichanot, A. and Roversi, P. (2001) Recovering experimental and theoretical electron densities in corundum using the multipolar model: IUCr multipole refinement project. Acta Crystallographica, A57, 290–303.

MANUSCRIPT RECEIVED AUGUST 2, 2009
MANUSCRIPT ACCEPTED AUGUST 20, 2009
MANUSCRIPT HANDLED BY BRYAN CHAKOUMAKOS